

Hole Injection and Electron Overflow Improvement in 365 nm Light-Emitting Diodes by Band-Engineering Electron Blocking Layer

This content has been downloaded from IOPscience. Please scroll down to see the full text.

2013 Jpn. J. Appl. Phys. 52 08JK05

(<http://iopscience.iop.org/1347-4065/52/8S/08JK05>)

View [the table of contents for this issue](#), or go to the [journal homepage](#) for more

Download details:

IP Address: 140.113.38.11

This content was downloaded on 25/04/2014 at 09:10

Please note that [terms and conditions apply](#).

Hole Injection and Electron Overflow Improvement in 365 nm Light-Emitting Diodes by Band-Engineering Electron Blocking Layer

Yi-Keng Fu^{1*}, Yu-Hsuan Lu², Rong Xuan^{1,3}, Jenn-Fang Chen³, and Yan-Kuin Su²

¹Electronics and Optoelectronics Research Laboratories, Industrial Technology Research Institute, Hsinchu 31040, Taiwan, R.O.C.

²Department of Electrical Engineering, Institute of Microelectronics, National Cheng Kung University, Tainan 70101, Taiwan, R.O.C.

³Electrophysics Department, National Chiao Tung University, Hsinchu 30010, Taiwan, R. O.C.

Received October 12, 2012; revised December 4, 2012; accepted December 19, 2012; published online May 20, 2013

The work reports a theoretical and experimental study on the device performance of near ultraviolet light-emitting diodes (LEDs) with specific design on the electron blocking layer (EBL) by employing the band-engineering. The simulation results show the polarization-induced downward band bending is mitigated in the specific EBL design and, hence, the capability of hole transportation increases and the behavior of electron overflow decreases. The experimental results show the LEDs with specific EBL design exhibited a reduction of forward voltage from 4.40 to 4.07 V and a much enhancement of light output power from 30.6 to 51.9 mW, compared with conventional LED.

© 2013 The Japan Society of Applied Physics

1. Introduction

Nitride-based light-emitting diodes (LEDs) in the ultraviolet (UV)-blue-green region of the spectrum have attracted more attention because of the versatile potential applications such as white-color lamps, full color display, environmental cleaning, biochemical processes and medical instruments.^{1,2)} UV LEDs operating in 365 nm is of special interest for data storage technology and biological applications, including UV light induced autofluorescence technique for detecting airborne pathogen.³⁾ For InGaN multi-quantum-well (MQW) LEDs, the electron blocking layer (EBL) is usually believed to be necessary. However, the effectiveness of using EBLs in InGaN LEDs is still debatable, because an EBL might act as a potential barrier for holes.^{4,5)} Therefore, use of an EBL, the injection of holes could be difficult owing to high effective mass, low mobility, low p-type doping efficiency, and downward band-bending induced by the serious polarization in the last-barrier/EBL interface.^{5,6)} In addition, it has been reported that the large polarization field in $\text{Al}_x\text{Ga}_{1-x}\text{N}$ EBL reduces the effective barrier height for electrons.⁷⁾ Therefore, the carrier overflow cannot be suppressed effectively. To reduce the polarization field in EBL, the polarization-matched EBLs (AlInN or AlInGaN) were proposed and demonstrated to be more effective in electron confinement.^{8,9)} However, it has difficulties of realization in epitaxy, and the crystal quality of the subsequent p-GaN layer will be degraded. More importantly, the hole injection cannot be improved effectively due to the existence of the ΔE_v between the last AlGaN barrier and EBL.⁷⁾ Recently, Kuo et al. have been reported some specific designs on the EBL of blue InGaN LEDs are investigated numerically in order to improve the hole injection efficiency without losing the blocking capability of electrons.¹⁰⁾ However, the similar structures can be used for near-UV LEDs are not clear. The effect of EBL structure with gradual Al composition from last barrier to EBL or EBL to p-type layer on hole injection efficiency and electron confinement is still unknown. In this study, we investigated the specific EBL designs for 365 nm LEDs numerically with the Simulator of Light Emitters based on Nitride Semiconductors (SiLENSe) simulation program in order to improve the efficiency of hole injection and reduce the electron overflow behavior. The numerical

simulations of band diagram, carrier distribution, radiative recombination rate were all executed to clearly look inside the experimental results. Then, it was realized by using metalorganic chemical vapor deposition (MOCVD), and the optoelectronic characteristics in LED with specific EBL designs was found to be much better than that in conventional LED with original EBLs.

2. Experimental Procedure

Samples used in this study were all grown on *c*-face (0001) 2-in. sapphire (Al_2O_3) substrates in a SR-4000 atmospheric pressure MOCVD system. Prior to the growth, we heated the substrate to 1100 °C in H_2 ambient to remove surface contamination. LED structure consists of a 20-nm-thick low temperature (LT) GaN nucleation layer, a 4- μm -thick Si-doped GaN n-cladding layer, an MQW active layer, a 25-nm-thick $\text{Al}_{0.3}\text{Ga}_{0.7}\text{N}$ EBL, and a 160-nm-thick Mg-doped $\text{Al}_{0.09}\text{Ga}_{0.91}\text{N}$ layer. The MQW active region consists of five periods of 3.0-nm-thick undoped $\text{In}_{0.02}\text{Ga}_{0.98}\text{N}$ well layer and 9-nm-thick undoped $\text{Al}_{0.17}\text{Ga}_{0.83}\text{N}$ barrier layer. The growth temperature of quantum well, quantum barrier, EBL and p- $\text{Al}_{0.09}\text{Ga}_{0.91}\text{N}$ layer are 840, 925, 1000, and 1000 °C, respectively. The LEDI denotes the original structure. The EBLs in structures B and C are divided into two independent layers. For LEDII, the 15-nm-thick of $\text{Al}_{0.3}\text{Ga}_{0.7}\text{N}$ EBL was grown, following to grow 10-nm-thick EBL with gradual Al composition from 30 to 9%. For LEDIII, the 15-nm-thick of $\text{Al}_{0.3}\text{Ga}_{0.7}\text{N}$ EBL was grown after growing 10-nm-thick EBL with gradual Al composition from 17 to 30%. The compositions of aluminum (Al) graded along the [0001] direction. The gradual Al composition was achieved by adjusting the trimethylaluminum flow rates. The trimethylgallium flow rates were fixed for the $\text{Al}_{0.17}\text{Ga}_{0.83}\text{N}$ barrier, EBL and p- $\text{Al}_{0.09}\text{Ga}_{0.91}\text{N}$ layer. We also prepared the bulk AlGaN layer was grown on the undoped GaN template in order to confirm Al composition of each AlGaN layers. These results are not shown here. The schematic diagrams of the original and specific structures were shown in Fig. 1. For the fabrication of LEDs, we first partially etched the surface of the samples until the n-type GaN layers were exposed. LEDs with indium tin oxide (ITO) serving as a transparent contact layer (TCL) were fabricated. We subsequently deposited Cr/Au onto the exposed n-type GaN layer to

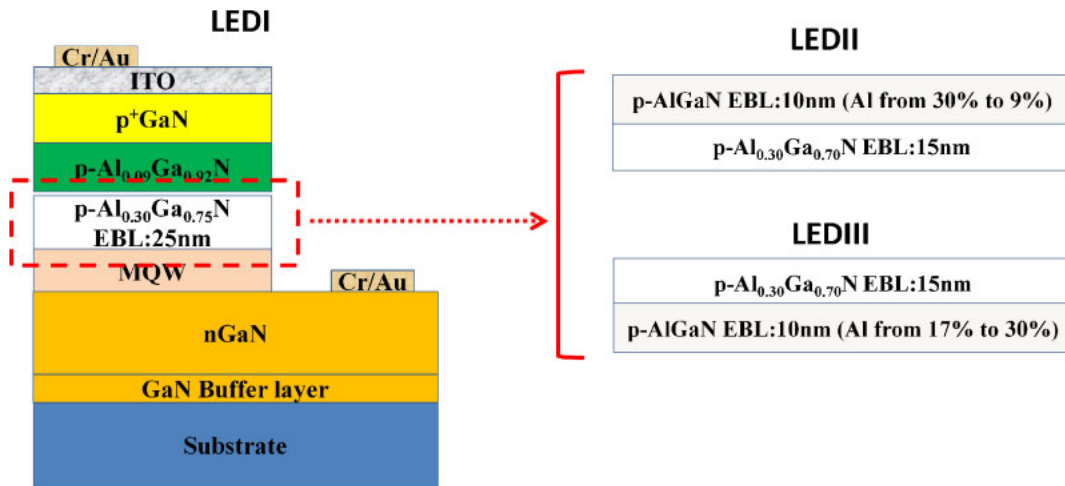


Fig. 1. (Color online) Schematic diagrams of the original structure and the structures with specific EBL design.

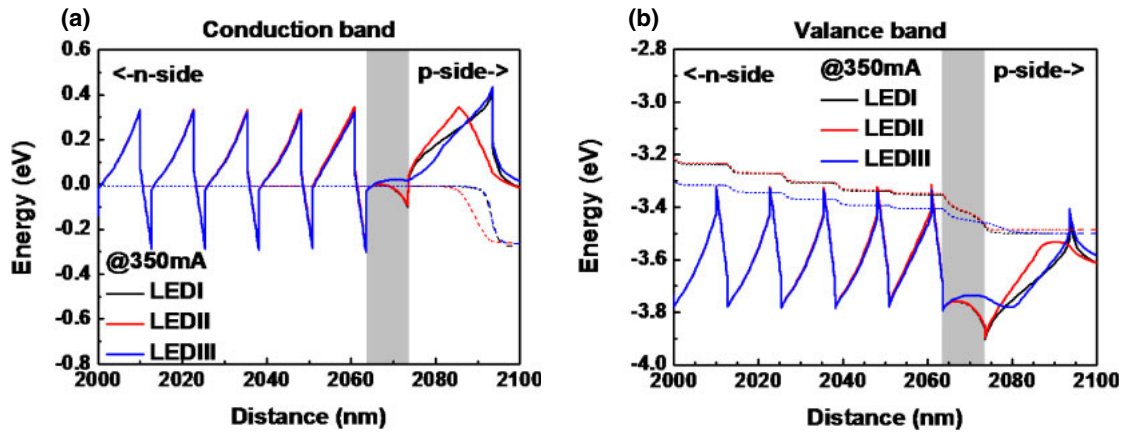


Fig. 2. (Color online) Calculated band diagrams of LEDs at 350 mA, (a) LEDI, (b) LEDII, and (c) LEDIII.

serve as the n-type electrode. The chip size of LEDs was $1000 \times 1000 \mu\text{m}^2$. Current–voltage (I – V) characteristics of the fabricated devices were then measured at room temperature by an HP4156 semiconductor parameter analyzer. The output powers were measured using the molded LEDs with the integrated sphere detector.

3. Results and Discussion

In order to investigate the physical mechanisms responsible for the improvement of light output intensity, numerical simulations of these LED structures with various EBL designs are performed using STR. SiLENSe 4.2 software.¹¹⁾ The simulated structures, such a layer thicknesses, doping concentrations, Al and In composition are the same as the actual devices and the corresponding nitride materials parameters are used in the calculations. Figures 2(a) and 2(b) are the calculated conduction and valence band diagrams of LEDI, II, and III at 350 mA current injection, respectively. The concept of band-engineering started from the observation on the band diagram of InGaN/AlGaN LEDs. For original LEDs operated under forward bias, the band diagram of EBL shows a triangular shape due to the internal polarization field and forward bias.¹²⁾ The valence band of EBL slopes upward from the n-GaN side toward the

p-GaN side, which retards the holes to transport across the triangular barrier. But if the composition of aluminum in EBL increases from the n-GaN side toward the p-GaN side, the band-gap broadens gradually. As a result, the barrier in the valence band could be level down, while the slope of the conduction band could be enhanced. The diffusion process for LEDIII is much easier than that for LEDI due to the flat valence band and much lower ΔE_v at the interface of the AlGaN barrier and EBL. The specific EBL design of LEDIII also has higher capability of electron confinement.

Figure 3 show the hole and electron concentrations within the active region of these three LED samples at 350 mA current injection, respectively. It can be clearly seen that the hole concentration decreases rapidly across the MQW region due to a potential spike at the interface between the last AlGaN barrier and the EBL in LEDI and II. The hole injection efficiency was enhanced by using specific EBL design because the situation of downward band-bending is mitigated. Moreover, the electron concentration in MQWs is also enhanced. This result indicates that specific EBL design can suppress the electron overflow out of active region more effectively than conventional EBL.

Figure 4(a) shows the calculated radiative recombination rates of these three LED samples at 350 mA. From the

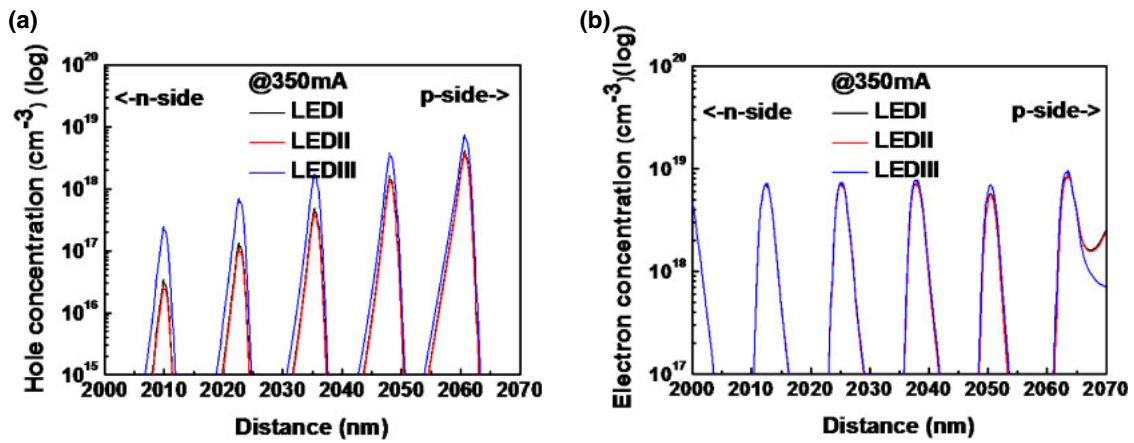


Fig. 3. (Color online) Calculated (a) hole and (b) electron concentrations of these three LEDs at 350 mA.

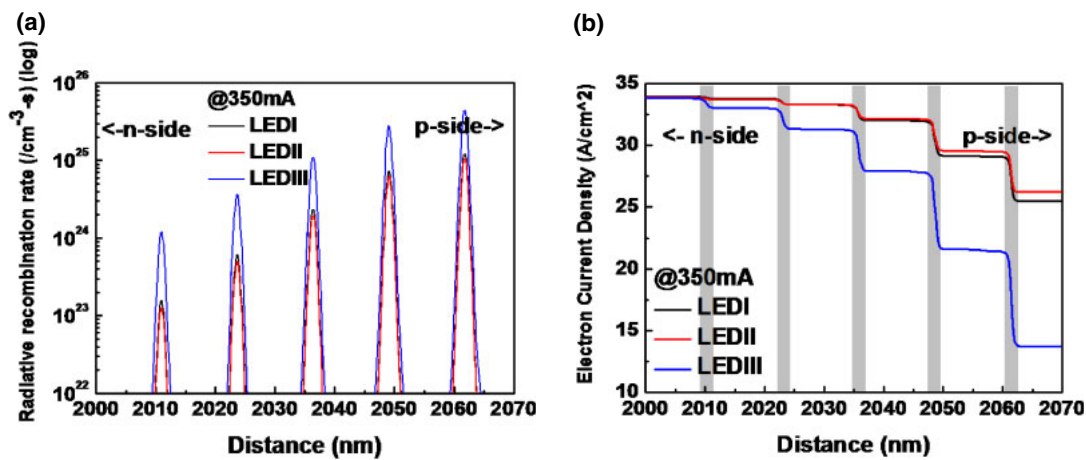


Fig. 4. (Color online) Calculated (a) the radiative recombination rates and (b) vertical electron current density profiles of these three LEDs at 350 mA current injection.

efficiency equation, the efficiency is increased with increasing the hole concentration (p) and bimolecular radiative recombination rate (B_{np}).⁷⁾ The increased bimolecular radiative recombination rate due to an increased hole concentration is the main reason for the higher EQE. Therefore, the specific design EBL for LEDIII exhibits much higher radiative recombination rate as compared to LEDI and LEDII because of more hole concentrations within the MQWs. Figure 4(b) shows the vertical electron current density profiles near the active regions of these three LEDs when the current injection is 350 mA. The positions of five QWs are marked with gray areas. The electron current is injected from n-type layers into QWs and recombines with holes. The electron current which overflows through QWs is viewed as leakage current. In Fig. 4(b), the electron leakage current is observed in all LEDs. After using specific EBL design, the electron overflow can be significant decreased. Therefore, the specific EBL design can provide the higher electron confinement to suppress the electron overflow.

Light-current-voltage ($L-I-V$) characteristics of these three fabricated LEDs are also plotted in Fig. 5. With 350 mA current injection, it was found that the forward voltages were 4.40, 4.25, and 4.07 V for LEDI, II, and III, respectively. The reduced V_f can be attributed to the improvement in hole

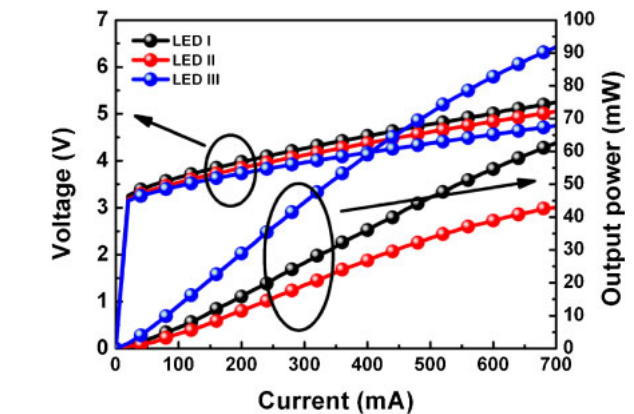


Fig. 5. (Color online) Forward voltage and output power as a function of injected current for these three LEDs.

injection and the higher-efficiency p-type doping in graded-composition EBL.¹³⁾ In the case of $L-I$ curves in Fig. 5, the output power of LEDI, II, and III at 350 mA current injection were 30.6, 23.2, and 51.9 mW, respectively. The lower output power of LEDII was attributed to the smaller effective barrier height of conduction band, compared with

LEDI. Therefore, the electron overflow of LEDII was more serious than that of LEDI, as shown in Fig. 4(b). The designed structures of EBL for LEDIII show significant improvement in light output power by 70%, compared with LEDI. The improved ratios at 700 mA are 1.92, 1.85, and 2.09 of their values at 350 mA. The larger improvement can be attributed to the situation of downward band-bending is mitigated at the interface of the last AlGaIn barrier and EBL, the hole injection efficiency increases markedly without losing the capability of electron confinement,¹⁴⁾ and the electron overflow was also reduced further by using the specific design of EBL.⁹⁾

4. Conclusions

In summary, the influence of polarization-induced downward band-bending in the last-barrier/EBL interface of 365 nm InGaIn/AlGaIn LEDs is investigated. The simulation results showed that the triangular barrier of conventional EBL at the valance band could be balanced, while the slope of the conduction band could be increased through the introduction of the specific design for the EBL. As a result, the hole concentration in MQWs was significantly increased, while better electron confinement was obtained. Furthermore, the electron overflow could be reduced markedly. Under 350 mA current injection, the forward voltage was reduced from 4.40 to 4.07 V and the output power can be enhanced by 70% by using the specific EBL design,

compared with LED with original EBL structure. Furthermore, we can improve the efficiency droop behavior. This work implies that carrier transportation behavior could be approximately modified by employing the concept of band-engineering.

- 1) H. Hirayama, N. Noguchi, S. Fujikawa, J. Norimatsu, N. Kamata, T. Takano, and K. Tsubaki: *Proc. SPIE* **7216** (2009) 721621.
- 2) H. Hirayama: *J. Appl. Phys.* **97** (2005) 091101.
- 3) A. Khan, K. Balakrishnan, and T. Katona: *Nat. Photonics* **2** (2008) 77.
- 4) M. F. Schubert, J. Xu, J. K. Kim, E. F. Schubert, M. H. Kim, S. Yoon, S. M. Lee, C. Sone, T. Sakong, and Y. Park: *Appl. Phys. Lett.* **93** (2008) 041102.
- 5) J. Lee, X. Li, X. Ni, Ü. Özgür, H. Morkoç, T. Paskova, G. Mulholland, and K. R. Evans: *Appl. Phys. Lett.* **95** (2009) 201113.
- 6) Y. K. Kuo, J. Y. Chang, M. C. Tsai, and S. H. Yen: *Appl. Phys. Lett.* **95** (2009) 011116.
- 7) S. H. Han, D. Y. Lee, S. J. Lee, C. Y. Cho, M. K. Kwon, S. P. Lee, D. Y. Noh, D. J. Kim, Y. C. Kim, and S. J. Park: *Appl. Phys. Lett.* **94** (2009) 231123.
- 8) S. Choi, H. J. Kim, S. S. Kim, J. Liu, J. Kim, J. H. Ryou, R. D. Dupuis, A. M. Fischer, and F. A. Ponce: *Appl. Phys. Lett.* **96** (2010) 221105.
- 9) Y. K. Kuo, M. C. Tsai, and S. H. Yen: *Opt. Commun.* **282** (2009) 4252.
- 10) Y. K. Kuo, J. Y. Chang, and M. C. Tsai: *Opt. Lett.* **35** (2010) 3285.
- 11) SiLENSe Physics Summary [<http://www.semitech.us/products/SiLENSe/>].
- 12) S. C. Ling, T. C. Lu, S. P. Chang, J. R. Chen, H. C. Kuo, and S. C. Wang: *Appl. Phys. Lett.* **96** (2010) 231101.
- 13) J. Simon, V. Protasenko, C. Lian, H. Xing, and D. Jena: *Science* **327** (2010) 60.
- 14) M. C. Tsai, S. H. Yen, and Y. K. Kuo: *IEEE Photonics Technol. Lett.* **22** (2010) 374.